

# Lung Field Segmentation

BMI 260 - Spring 2017

Yusuf Roohani

yroohani@stanford.edu

**Abstract.** With the recent growth in availability of affordable imaging systems and the number of patients being prescribed a CT scan, there has been a proportional increase in the amount of data that these machines generate. Automated processing of these images is a non trivial problem and would prove tremendously valuable both for clinicians and researchers. Segmentation forms the first critical step in this procedure and approaches towards automating it have been extensively studied for the past few decades. Recent advancements in the field of computer vision and machine learning have further accelerated these efforts. In this study, we apply a simple yet reliable and transparent approach to this problem. CT scans from 19 patients obtained from the Data Science Bowl 2017 competition were used for designing the algorithm. The images were first segmented using an Otsu threshold applied to a range of interest within the standardized hounsfield units. A morphological transformation was applied to reduce noise followed by a connectivity based region proposal method to isolate different regions. Regions along the border were discarded and a volume based threshold was applied to remove left-over noise. Visualizations were obtained using matplotlib and Fiji. The results appear to be very satisfactory with scope for improvement in the smoothness of the lung segments. Since speed was claimed as one of our strengths, we also recognize several obvious shortfalls in computational efficiency that can also be addressed in future.

## 1 Introduction

Computed tomography scanning (CT) is a widely used medical imaging modality. It is employed in a variety of diagnostic applications including tumor localization, anatomical mapping and stereotactic surgery planning [1]. CT usage has increased 20-fold in the US over the past two decades. [7]. This has been fueled by the growing interest in screening of asymptomatic patients for timely diagnosis of several conditions, one of which is early stage lung cancer.

The image acquisition procedure for a CT scan involves generating a series of two dimensional cross sectional images, generally using X-rays. These are then stacked one on top of another to generate a three dimensional visualization of the subject's anatomy. Thus, CT scanners generate large volumes of data which must undergo several computational processing steps for extraction of valuable information. It is perhaps only surpassed in its information content by the MRI, although CT scans are less costly and quicker [1].

Automating the analysis of this data has turned into a very active area of research within the field of medical imaging [6]. There are several algorithms which aim to automate the processing of CT scans. Within these analyses, segmentation generally forms a critical first step. For instance, Armato et al. [8] illustrated the importance of accurate lung segmentation through a significant improvement in automated nodule detection.

Since the lungs are essentially composed of air, they show up as a different color within the scan as compared to the rest of the body. This forms the basis for most segmentation approaches [6]. Many of these use some form of thresholding, the crudest of which could be as simple as applying a pre-defined range of interest in standardized hounsfield values. One approach well suited for this problem is Otsu's method - this involves selecting an optimum binary threshold such that the variance on either side of the threshold is suitably minimized. This is normally used along with region growing methods such as connectivity component labeling to clearly isolate distinct regions. [10] Finally, morphological transformations such as dilation and erosion are performed to smoothen out rough edges and noise. Hole filling is also often attempted using connectivity graphs. [11]

Machine learning algorithms such as k-means and support vector machines are another family of approaches used for segmentation. They also result in a pixel value based decision boundary but these can easily be extended beyond binary problems, which is not as straightforward with Otsu's method. More recently, supervised techniques such as convolutional neural networks have seen a tremendous growth due to their high accuracy. In [4], Cha et al. use deep neural network architectures to distinguish between the inside and the outside of the bladder. The drawbacks of these methods is the large size of training datasets required with manual annotation and increased computational resource. Another pitfall is the lack of transparency.

Further fine tuning of segmentation results can be performed using structural and anatomical data. For instance 'air-like' regions outside the body cavity, i.e. near the edges of the scan, must necessarily not be part of the lung and can be removed.

Some of the challenges still faced in this field are accounting for pathologies in the lung that can alter this clear threshold [6]. Developing a robust segmentation method that is accurate to noise and variability in scanning procedure or other artifacts would be very valuable for gaining the confidence of clinicians.

After completing the actual segmentation, it is also important to develop an approach that accurately and realistically visualizes the results of the segmentation. One popular approach within this area is the marching cubes method. It can convert a 3D image volume into a mesh surface [3].

For this project, we started by using a standard Otsu based threshold coupled with connectivity map based region growing. We rejected all regions that were in contact with the edges. We also used morphology operations (dilations followed by erosion) to reduce noise. All these operations were performed in 2D. Finally to remove any external organs or other noise that may have also been included

in the segmentation we applied a volume threshold in 3D. 3D visualization was performed using both matplotlib and Fiji. CT scans from 10 patients were used for validation.

## 2 Data

The data for this study was provided by the website Kaggle as part of the 'Data Science Bowl 2017' [2]. The data consists of CT images of the lung for several patients. There are multiple axial slices of the chest cavity for each patient. Fig.1 shows a sample 2D slice from this dataset. Fig.2 shows the full series of slices for a given patient. Relevant information about each image such as its location and the hounsfield normalization parameters are provided in the header file. Each image has a resolution of 512x512 pixels and the values generally range from -2000 to 2000.

## 3 Methods

### 3.1 Studying dataset

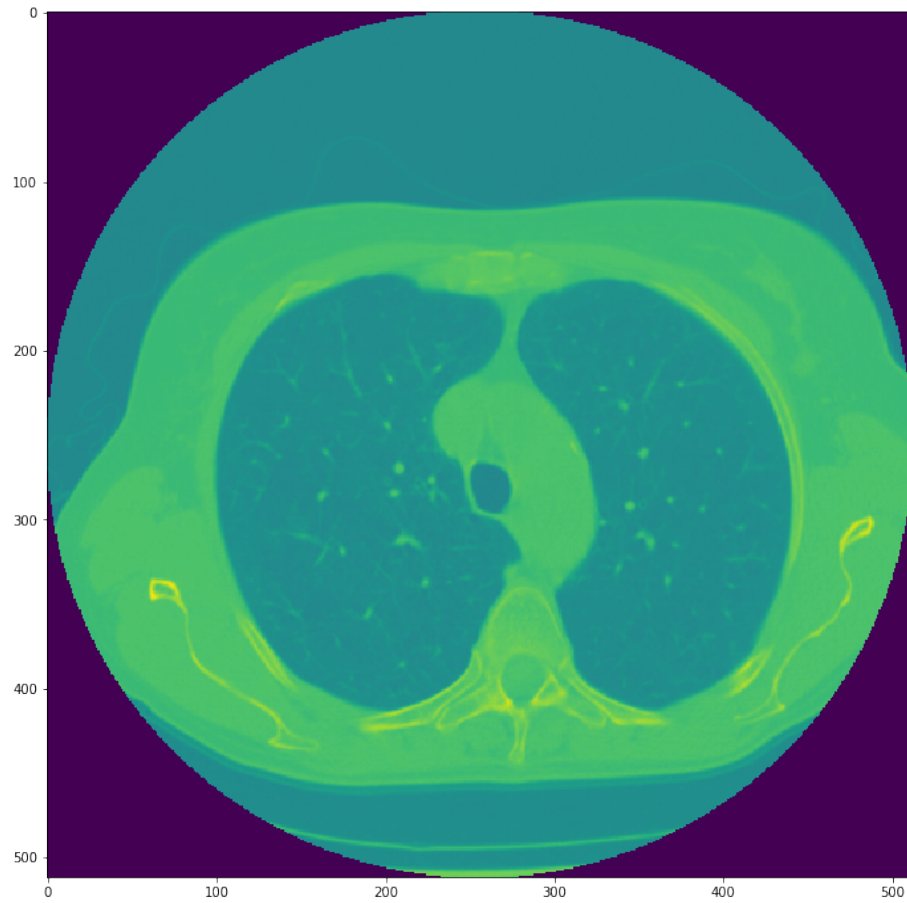
The first step was to look at the images and try to visualize the best means of discriminating between different regions.

Fig. 2 shows lung scans at different locations for a given patient. These have been arranged in sequential order using the information attached within the DICOM format. It's clear that the sections proceed from the trachea right down to the base of the lungs. Near the bottom they also capture some other organs.

We can see that, in general, the scans tend to follow a common pattern where the lung sections are captured within a circular region which represents the body cavity. Since the lungs are mainly composed of air, we can see that the level of signal attenuation within the lungs is similar to that seen outside the body cavity, yet very different from that within the body itself. This makes our work easier as the region within the body external to the lungs can easily be distinguished. At the same time, that outside the body is also clearly distinct from that within the lungs.

### 3.2 Normalizing data

The pixel values for these scans were arbitrary values within the range of [-2000, 2000]. In terms of hounsfield units in particular, we were interested in a small range around 500. So, in order to make a clearer distinction between the lung and the rest of the organs in the body which occupy a different position on the hounsfield scale of radiodensity, we applied an upper threshold of -400 beyond which everything was clubbed under the same value. The goal was to make it easier to make a binary distinction between lung and everything else. We also removed all values below an arbitrarily small threshold of 0.05, so as to prevent skewing of the variance of the lung class.



**Fig. 1.** Sample image from the Kaggle Data Science Bowl 2017 dataset consisting of CT scans of lungs

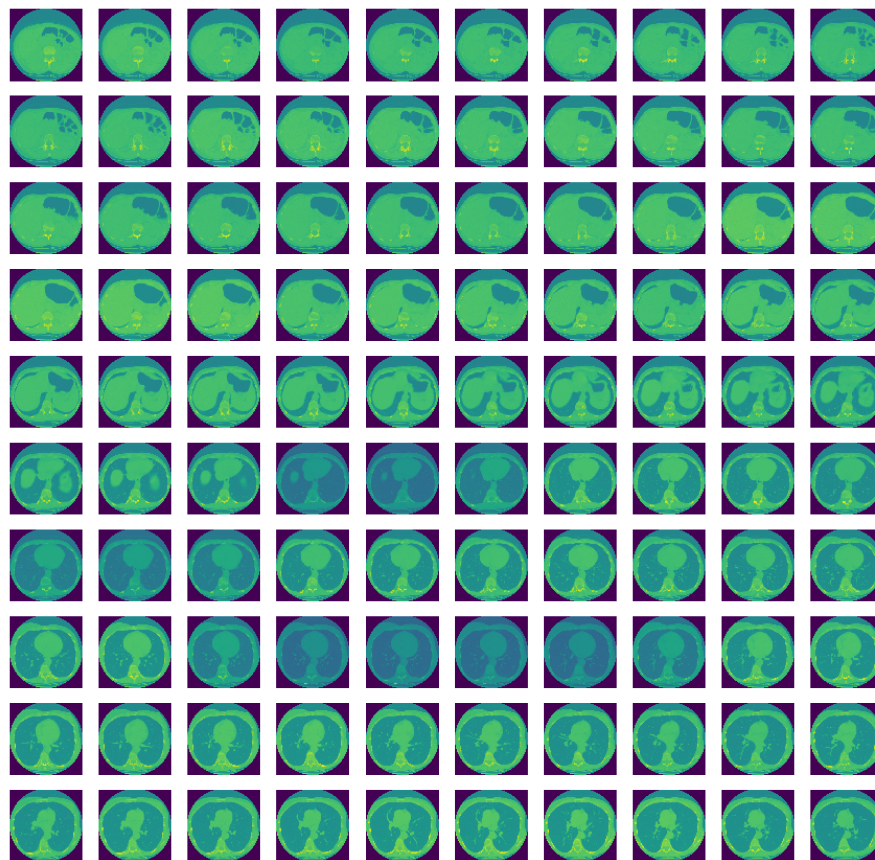


**Fig. 2.** Full image sequence from a single patient from the Kaggle Data Science Bowl 2017 dataset

Standardizing the pixel values to hounsfield units is a linear transformation and would not effect relative differences in any way. However using the hounsfield units to set a maximum threshold is not a linear function and has a significant impact on the output of segmentation. For simplicity in analyzing histograms, we normalized the range to lie between 0 and 1. This was done by subtracting the minimum and dividing by the maximum.

### 3.3 Segmentation

The first step in our approach was to look at the histogram of pixel values. This was easy to implement since this is only a single channel image. The histogram (Fig 9b) looked perfect for the application of Otsu’s threshold. This technique splits the data into two clean sections such that the variance within either set is minimized. We see a clear bimodal distribution between -1000 and 1000 and the variance is very similar too. The two peaks represent pixels within the lung and those representing the body cavity. Thus, applying this threshold should give us a clean split between the regions we are most interested in discriminating between.

Fig 3 show the thresholded image after the application of the threshold. There appear to be several gaps in the lung that is likely due to the change in radiodensity within the blood vessels. Theoretically, these should also form part of the lung segmentation, so we tried to close some of the contours using morphological transformations. We specifically used a technique called closing which is a mixture of dilation followed by erosion.

We now use a simple region growing procedure to identify connected regions in an image. This works especially well for a binary image like ours since it is very straightforward to identify connected regions using a connectivity graph. We use the default setting of looking only 1 pixel ahead within a neighborhood of 8 pixels. Thus, we are quickly able to isolate the lungs. We can also now remove the empty space surrounding the body since it must necessarily be disconnected from the lungs. To do this, we simply get rid of any region that is in contact with an edge of the image. As for the body cavity, we assign it the value of a background pixel, so it is also not considered in the region proposal algorithm.

We are finally left with the lungs and some noise around the lungs (Fig 4). We can reduce the noise by setting a volume threshold since the volume capture by the lungs themselves is always much larger. Notice that at this point the thresholding will happen in 3D, since thresholding by area can be risky due to the variability in the area of different lung slices. The graph in Fig. 4 shows the region volume for the lung region compared with that for the next largest region. We used this to determine an optimal volume threshold.

### 3.4 3D visualization

For the 3D visualization, we first stacked up all the segmented lung image slices in the correct order. Using a simple contour function, we could trace out the

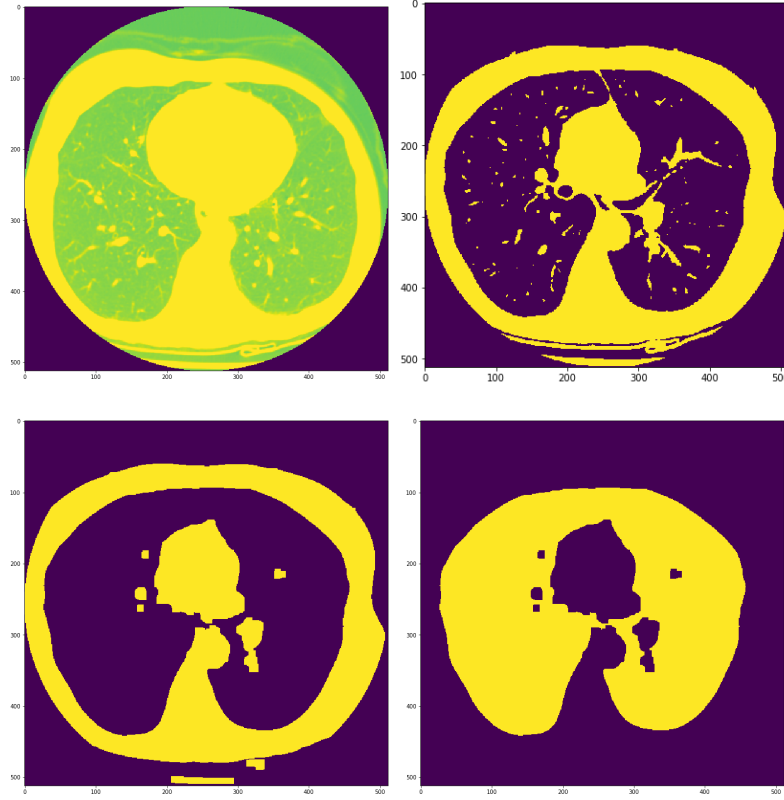


**Fig. 3.** After the application of the Otsu threshold, we applied morphological closing (i.e. dilation followed by erosion) to close up the gaps. We then used a connectivity map to mark out distinct regions and removed any region in contact with the edges of the image

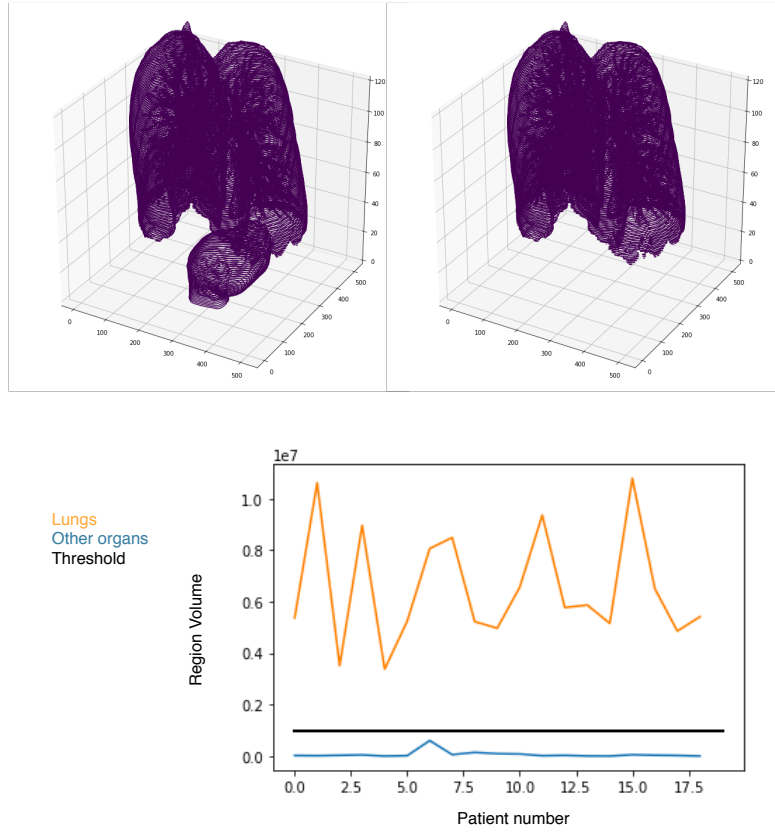


**Fig. 4.** After performing area based thresholding, volume based thresholding was performed to remove noise such as other organs that may have been picked up during the CT. On the left is the image before applying a volume threshold and on the right is after its application. The threshold was calculated by running the volume based region proposal algorithm for 19 patients and seeing what worked best



outlines of the lungs at each slice level. This resulted in something roughly approximating a 3D volume.

To get a more elegant visualization of the lungs, we employed a marching cubes algorithm to fill draw a 2D surface mesh around this volume. This algorithm creates a polygonal representation of constant density surfaces from a 3D array of data [3]. We first tried using matplotlib but the rendering was taking far too long (~1.5 hour for one image), so we ended up using Fiji instead. An added advantage of using Fiji was that it's easier to manipulate image and look at it from different angles.

## 4 Results

Fig 5 shows the results of the slice specific segmentation. Fig.6 shows the segmentation results for the entire lung for 10 different patients. Fig. 7 and Fig. 8 show the 3D rendering using Fiji. The results are quite satisfactory given the simplicity of the algorithm and the speed with which it is able to perform segmentation. None of the lungs look deformed and there are no external organs being added to the image. There is of course noise around the edges of the lungs and some misshapen contours around the interior of the central section.

## 5 Discussion

Studying our approach right from the start, we did an analysis on decision to use hounsfield thresholding (Fig. 9). Since we intended to apply an Otsu threshold as the next step, the sharp change in hounsfield values was creating far too steep of a gradient in the variance to the right of the Otsu threshold. Thus, as we can see from the histograms nothing except the peak that we defined manually was being allotted a distinct class, and so we had essentially reduced the effectiveness of the Otsu threshold. Due to shortage of time we haven't changed our algorithm to reflect the more accurate method. While the noise was mostly made up for using the morphological transformation (closing), a larger kernel size would've eased it out even more.

Approaching the segmentation as a volume based approach right from the start may have saved time and unnecessary computation. As we can see from the slices, another organ (looks like the heart) also got added to the lung segmentation. This had to be thresholded out using a volume based region proposal. A single call to such a region proposal, as opposed to doing two (one based on area and the other on volume) would've been more efficient, with similar accuracy.

While validation was performed using 10 different patients, these were not a distinct set from what was used to derive model parameters such as the volume threshold. This is a flawed approach to designing a robust segmentation algorithm, as training and validation sets should ideally be kept distinct.



**Fig.5.** This is the output of the segmentation algorithm on the same image set as Fig 1. These are all binary images. Notice the presence of an abnormal organ in the first few rows. This organ could not be segmented out at the slice level and had to be removed later through volume thresholding

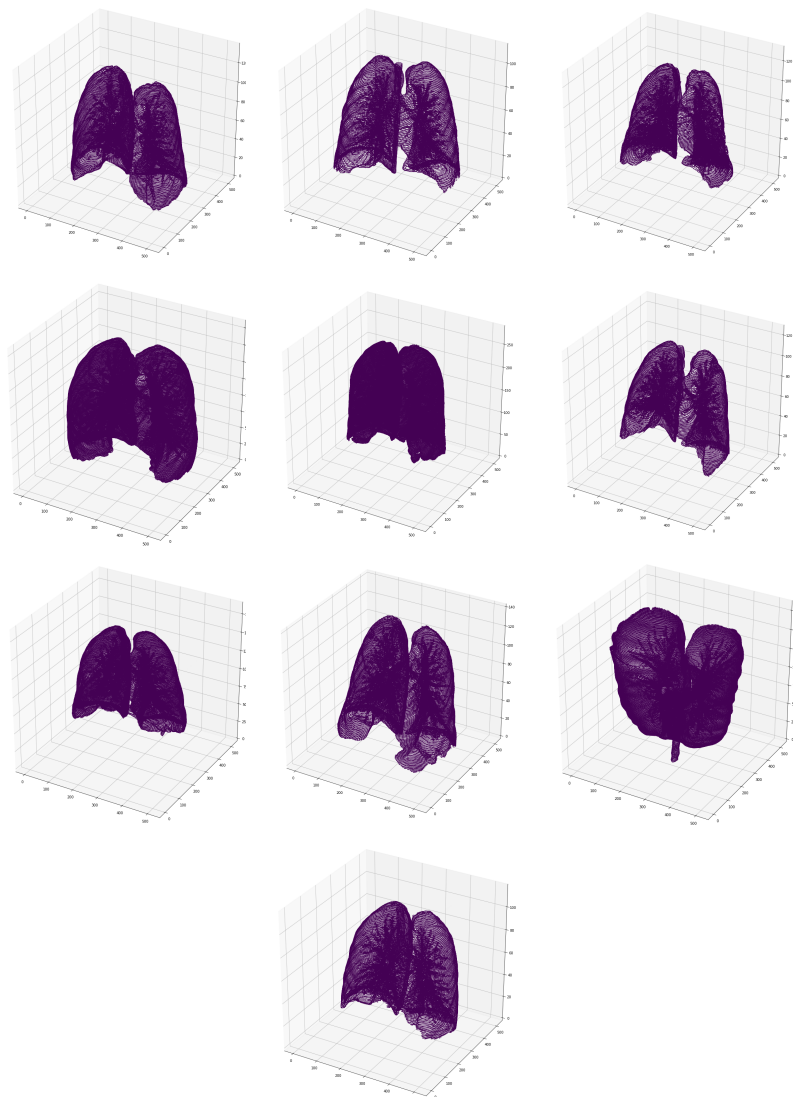


**Fig.6.** This is a 3D visualization using the 3D contour function in matplotlib. It is clear from all the images that the algorithm is able to segment out the lung reasonable well. It's still a little rough around the edges and this is noticeable near the bottom of the lungs and in the central region (not visible here). There is also an increase in opacity in case of lungs segments that are more closely spaced which is a consequence of the simplified contour based approach.

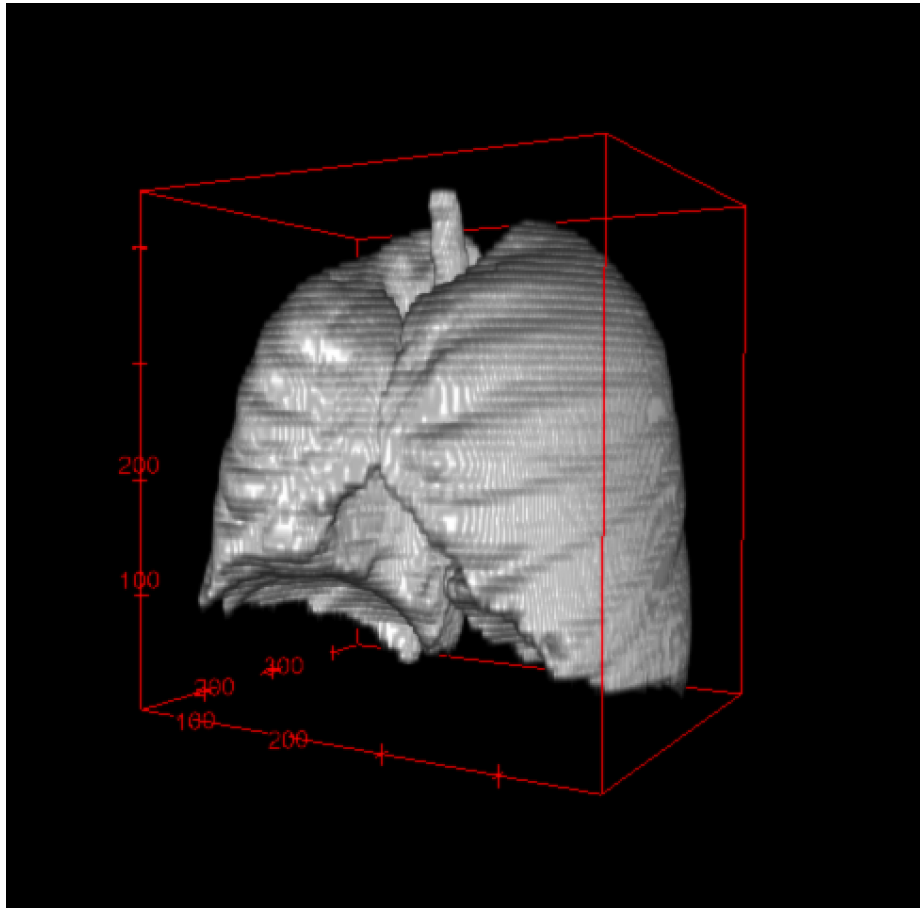


**Fig. 7.** This is a sample 3D visualization using Fiji. One can clearly see that the algorithm captures the full structure of the lungs quite well. There is some noise visible near the lower edges.

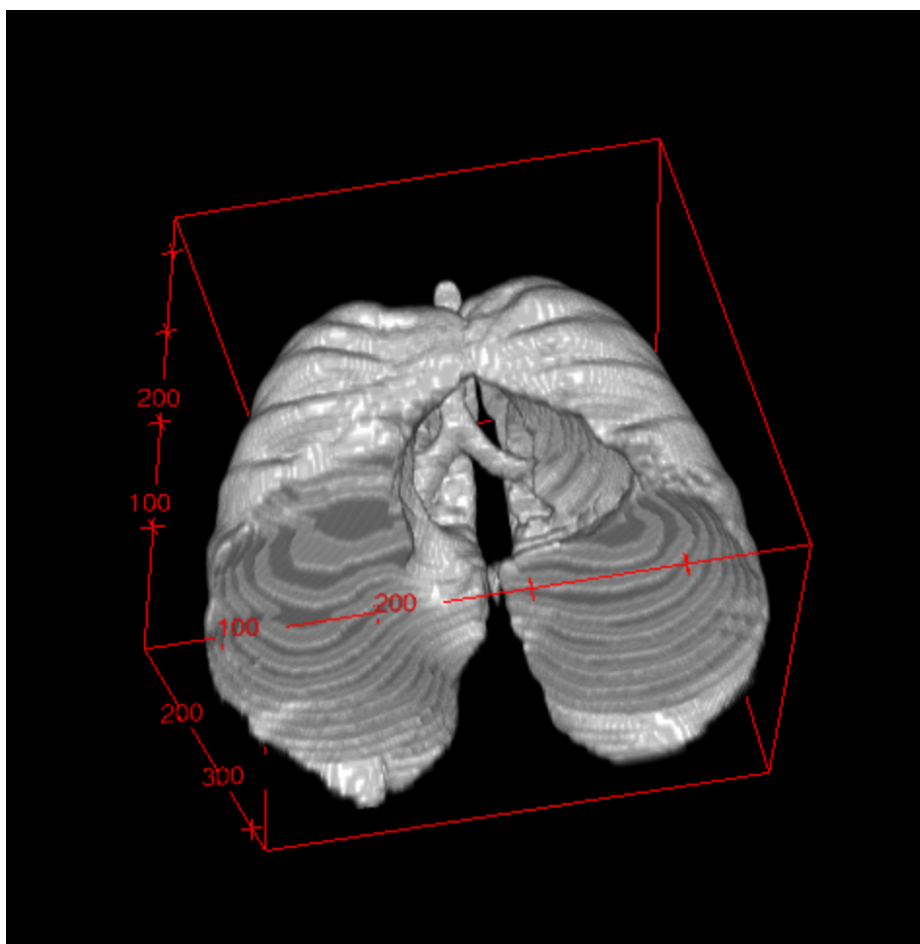


**Fig. 8.** This is the same 3D visualization from Fiji but at a different angle. The noise in the central structures around the bronchi are more clearly visible here.

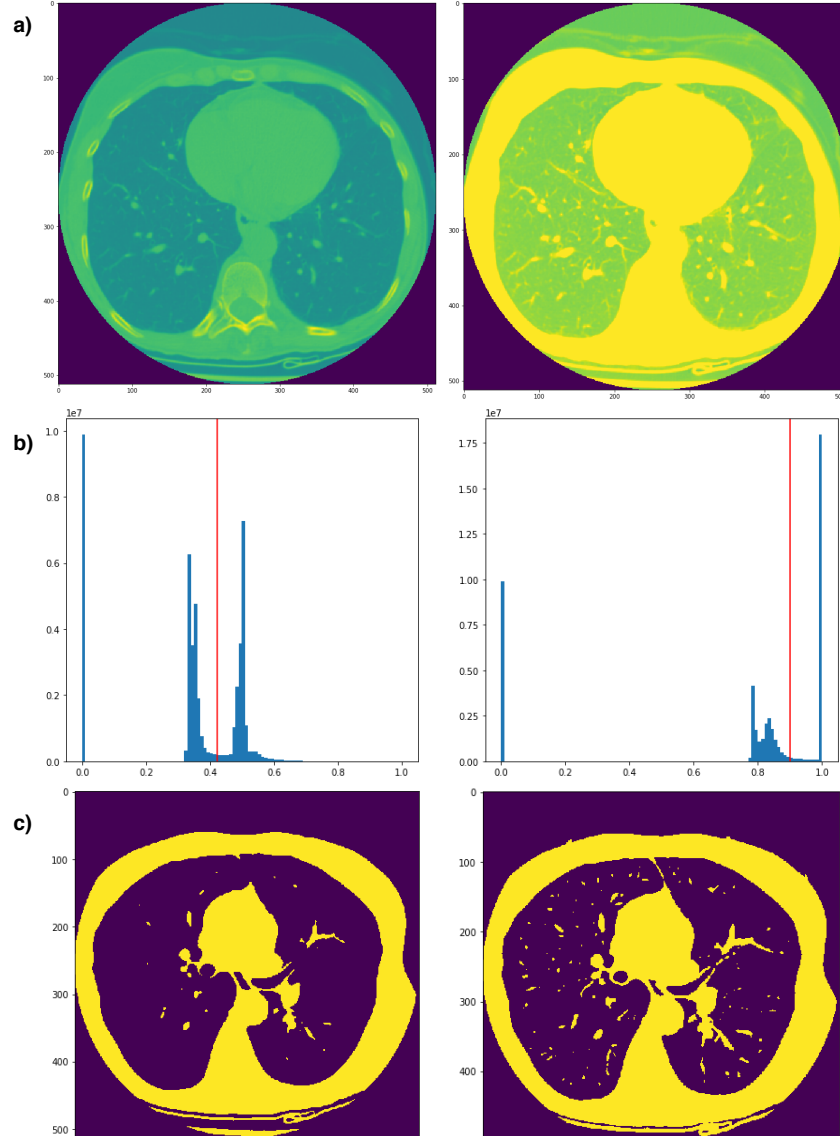


**Fig. 9.** Comparing the effect of Otsu thresholding before and after applying a Hounsfield pixel range to the image. (a) Effect of applying a maximum hounsfield unit threshold of -400 to the image. (b) Change in the histogram for the image after the application of the threshold. (c) Effect of applying Otsu's threshold on either image. We can clearly see that there is increased fragmentation in the image on the right.

## References

1. Acharya, Raj, et al.: Biomedical imaging modalities: a tutorial. *Computerized Medical Imaging and Graphics* 19.1 (1995): 3-25.
2. Data Science Bowl 2017 <https://www.kaggle.com/c/data-science-bowl-2017>
3. Lorensen, William E., and Harvey E. Cline.: Marching cubes: A high resolution 3D surface construction algorithm. *ACM siggraph computer graphics*. Vol. 21. No. 4. ACM, 1987.
4. Cha, Kenny H., et al. Urinary bladder segmentation in CT urography using deep?learning convolutional neural network and level sets. *Medical physics* 43.4 (2016): 1882-1896.
5. <https://www.raddq.com/dicom-processing-segmentation-visualization-in-python/>
6. Sluimer, Ingrid, et al.: Computer analysis of computed tomography scans of the lung: a survey. *IEEE transactions on medical imaging* 25.4 (2006): 385-405.
7. Hall, E. J., and D. J. Brenner.: Cancer risks from diagnostic radiology. *The British journal of radiology* (2014).
8. Armato III, Samuel G., et al.: Lung image database consortium: Developing a resource for the medical imaging research community 1. *Radiology* 232.3 (2004): 739-748.
9. Van Rikxoort, Eva M., et al.: Automatic segmentation of pulmonary segments from volumetric chest CT scans. *IEEE transactions on medical imaging* 28.4 (2009): 621-630.
10. Hu, Shiyong, Eric A. Hoffman, and Joseph M. Reinhardt.: Automatic lung segmentation for accurate quantitation of volumetric X-ray CT images. *IEEE transactions on medical imaging* 20.6 (2001): 490-498.
11. Wang, Jiahui, Feng Li, and Qiang Li.: Automated segmentation of lungs with severe interstitial lung disease in CT. *Medical physics* 36.10 (2009): 4592-4599.